

## Stability of Crystal Lattices\*

DUANE C. WALLACE AND JANICE L. PATRICK

*Sandia Laboratory, Albuquerque, New Mexico*

(Received 1 May 1964; revised manuscript received 31 August 1964)

The condition that a given lattice model be stable against all small deformations is that all the eigenvalues of all the dynamical matrices be positive. The stability of several lattices is studied by calculating the dynamical matrices for a large number of wave vectors in the Brillouin zone. Central potential interactions represented by Lennard-Jones and Rydberg forms are used, and the nearest-neighbor distance  $\epsilon$  is allowed to vary throughout a range of  $\pm 10\%$  of the value  $\epsilon_0$  which minimizes the static lattice potential. The fcc and hcp lattices are stable for all central potentials and all values of  $\epsilon$  studied; the bcc is stable for all values of  $\epsilon$  for long-range central potentials; and the diamond is stable for a range of  $\epsilon > \epsilon_0$  for all central potentials studied. The sum of the static lattice-potential plus the harmonic zero-point energy is minimized as a function of  $\epsilon$ , and it is found for all stable models except diamond that this procedure increases  $\epsilon$  from  $\epsilon_0$  by about  $\epsilon_0\kappa$ , where  $\kappa = \hbar/M^{1/2}D^{1/2}\epsilon_0$ , with  $M$  = mass of ions and  $D$  = static lattice binding energy. For diamond, however, there is no minimum in the range of  $\epsilon$  for which the lattice is stable, for physically reasonable values of  $\kappa$ . Born has suggested that if a lattice is stable for long waves, it is stable for short waves; a counterexample has been found in the present study for the diamond lattice. A comprehensive table of accurate lattice sums is given in an Appendix.

### I. INTRODUCTION

THE problem of the stability of crystal lattices has been extensively investigated by Born and other workers.<sup>1-6</sup> In these studies, the lattice was considered to undergo a homogeneous deformation, and the elastic-energy density was expanded in a series up to second order in the deformation parameters. The equilibrium condition was that the elastic energy density be stationary with respect to the deformation parameters, and the stability condition was that the elastic-energy density, evaluated at equilibrium, be a positive definite quadratic form.

The present study of lattice stability is based on the requirement that if the lattice is to be stable against all small deformations, all normal-mode frequencies must be real. Born and Huang<sup>4</sup> have pointed out that the stability against homogeneous deformations insures only that the long-wavelength modes have real frequencies. It has been shown that the stability against all deformations follows from the stability against homogeneous deformations for a linear chain model<sup>1</sup> and also for a fcc model with nearest-neighbor interactions.<sup>3</sup> In the present work the dynamical matrices of the harmonic lattice-dynamics problem were calculated for a large number of points in the Brillouin zone, for fcc, bcc, dia (diamond), and hcp lattices for models based on two-body central forces, and these matrices were checked for positive eigenvalues.

It has been shown<sup>7</sup> that the condition that the elastic-energy density be stationary with respect to the deformation parameters is equivalent to the Born and Huang<sup>4</sup> infinite-lattice condition that the stresses must vanish in the equilibrium configuration. In either form, this equilibrium condition is needlessly restrictive; indeed, if the lattice structure and the interatomic potentials are specified, the application of this condition fixes the value of the unit cell volume. By explicitly including externally applied forces in the lattice Hamiltonian, it is possible to extend lattice dynamics, and also the method of homogeneous deformation, to the case of a crystal in a state of arbitrary initial elastic strain.<sup>7</sup> In this case the only equilibrium condition is that the net force on each ion must vanish in the equilibrium configuration. For the lattice models considered in the present paper, this equilibrium condition is satisfied by symmetry (with the neglect of surface effects), and hence is satisfied for any value of the unit cell volume. In contrast to the previous studies, in which the unit cell volume was considered fixed,<sup>1-6</sup> the present work investigates the stability over a wide range of unit cell volume.

### II. METHOD OF CALCULATION

#### Dynamical Matrices

The potential energy due to the interactions among the ions in a large finite crystal may be expanded as

$$U(\mathbf{r}_{nj} + \mathbf{u}_{nj}) = U(\mathbf{r}_{nj}) + \sum_{n,\rho} X_{n\rho} \mathcal{U}_{n\rho} + \frac{1}{2} \sum_{nn',\rho\rho'} A_{n\rho,n'\rho'} \mathcal{U}_{n\rho} \mathcal{U}_{n'\rho'} + \dots \quad (2.1)$$

Here and in the following the notation is the same as that used previously.<sup>8,9</sup> The symbol  $n$  labels a unit cell,

<sup>7</sup> D. C. Wallace, Rev. Mod. Phys. (to be published).

<sup>8</sup> D. C. Wallace, Phys. Rev. **131**, 2046 (1963). Two typesetting errors have occurred in this paper. In (3.15) the inequality for  $p_2$  should read  $0 \leq p_2 \leq \frac{1}{2}P$ . Equation (4.9) should read

$$\Omega = [2\alpha\beta D/3e^2(\alpha-\beta)] [(\alpha-1)S_{\alpha-1}S_{\alpha+2} - (\beta-1)S_{\beta-1}S_{\beta+2}].$$

<sup>9</sup> D. C. Wallace, Phys. Rev. **133**, A153 (1964).

\* This work was supported by the U. S. Atomic Energy Commission.

<sup>1</sup> M. Born, Proc. Cambridge Phil. Soc. **36**, 160 (1940); **38**, 82 (1942); M. Born and R. Furth, *ibid.* **36**, 454 (1940).

<sup>2</sup> R. D. Misra, Proc. Cambridge Phil. Soc. **36**, 173 (1940); M. Born and R. D. Misra, *ibid.* **36**, 466 (1940).

<sup>3</sup> S. C. Power, Proc. Cambridge Phil. Soc. **38**, 61 (1942); H. W. Peng and S. C. Power, *ibid.* **38**, 67 (1942).

<sup>4</sup> M. Born and K. Huang, *Dynamical Theory of Crystal Lattices* (Clarendon Press, Oxford, 1954).

<sup>5</sup> L. A. Girifalco and V. G. Weizer, Phys. Rev. **114**, 687 (1959).

<sup>6</sup> Y. P. Varshni and F. J. Bloore, Phys. Rev. **129**, 115 (1963).

$j$  labels an ion in a unit cell,  $i$  labels a Cartesian coordinate,  $\nu$  stands for a pair of indices  $(n, j)$ , and  $\rho$  stands for a pair of indices  $(j, i)$ . There are  $J$  ions per unit cell,  $M_j$  is the mass of an ion of type  $j$ , and  $M_c$  is the total mass of ions in one unit cell. The equilibrium position of ion  $(n, j)$  is  $\mathbf{r}_{nj} = \mathbf{r}_n + \mathbf{r}_j$ , and the displacement of ion  $(n, j)$  from its equilibrium position is  $\mathbf{u}_{nj}$ .

The criterion for a given lattice model to be stable against all small deformations is that all of the normal-mode frequencies are real. For this study it is not necessary to take explicit account of the anharmonic terms in the potential energy, and the harmonic Hamiltonian may be used. In the presence of externally applied forces  $\mathbf{f}_{nj}$  [each  $\mathbf{f}_{nj}$  is applied to ion  $(n, j)$ ], the harmonic Hamiltonian is<sup>7</sup>

$$\mathcal{H} = U(\mathbf{r}_{nj}) + \frac{1}{2} \sum_{n, \rho} M_j (\dot{u}_{n\rho})^2 + \sum_{n, \rho} (X_{n\rho} - f_{n\rho}) u_{n\rho} + \frac{1}{2} \sum_{nn', \rho\rho'} A_{n\rho, n'\rho'} u_{n\rho} u_{n'\rho'}, \quad (2.2)$$

where  $\dot{u}_{n\rho}$  is the time derivative of  $u_{n\rho}$ . The equilibrium condition is

$$X_{n\rho} - f_{n\rho} = 0, \quad \text{all } (n, \rho). \quad (2.3)$$

The present work is restricted to the case of isotropic surface forces; hence the  $\mathbf{f}_{nj}$  are applied only to the ions at the surface of the crystal. In the interior of the crystal, i.e., farther from the surface than the range of the interatomic forces, the lattice is presumed to be perfectly periodic with constant unit cell volume. The normal coordinates of (2.2) are found, with an error corresponding to the neglect of surface effects, by applying the cyclic boundary condition to macrocrystals in the interior of the large finite crystal.<sup>7</sup> Since the  $\mathbf{f}_{nj}$  vanish in the interior, the equilibrium condition (2.3) becomes

$$X_{n\rho} = 0, \quad \text{all } (n, \rho) \text{ in the interior.} \quad (2.4)$$

The normal coordinates are enumerated by the wave vectors  $\mathbf{k}$  and the polarization index  $s$ . If the macrocrystals contain  $N$  unit cells, there are  $N$  values of  $\mathbf{k}$  distributed uniformly over the first Brillouin zone, and there are  $3J$  values of  $s$  associated with each  $\mathbf{k}$ . The circular frequencies  $\omega_{\mathbf{k}s}$  of the normal modes are related to the eigenvalues  $\eta_{\mathbf{k}s}$  of the dynamical matrices ( $\mathbf{a}_{\mathbf{k}}$  matrices) by

$$M_c (\omega_{\mathbf{k}s})^2 = \eta_{\mathbf{k}s}, \quad (2.5)$$

where

$$a_{\mathbf{k}, \rho\rho'} = \sum_{n'} A_{n\rho, n'\rho'} \exp[-i\mathbf{k} \cdot (\mathbf{r}_{nj} - \mathbf{r}_{n'j'})], \quad (2.6)$$

$$\sum_{\rho} M_j v_{\mathbf{k}, \rho s} v_{-\mathbf{k}, \rho s'} = M_c \delta_{ss'}. \quad (2.7)$$

Equation (2.7) represents the orthonormalization of the components  $v_{\mathbf{k}, \rho s}$  of the eigenvectors of  $\mathbf{a}_{\mathbf{k}}$ . The condition for lattice stability is

$$\eta_{\mathbf{k}s} > 0, \quad \text{all } (\mathbf{k}, s). \quad (2.8)$$

The static lattice potential  $U(\mathbf{r}_{nj})$  is taken to be  $N$  times the potential of one unit cell in the interior due to interaction among the ions. The effect of isotropic surface forces is taken into account by allowing the unit

cell volume to vary.  $U(\mathbf{r}_{nj})$  and the coefficients  $X_{n\rho}$ ,  $A_{n\rho, n'\rho'}$  are functions of the unit cell volume. The volume dependence of  $A_{n\rho, n'\rho'}$  arises implicitly from anharmonic terms in the potential energy; the allowance of this volume dependence, and the corresponding volume dependence of the normal-mode frequencies, without explicit inclusion of higher order terms in the potential energy, represents the quasiharmonic approximation.

It is convenient to take the nearest-neighbor distance  $\epsilon$  as the variable which represents the unit cell volume. Define  $\sigma$  as

$$\sigma = (\epsilon - \epsilon_0) / \epsilon_0, \quad (2.9)$$

where here, and in the following, a subscript 0 means that a quantity is to be evaluated at the value of  $\epsilon$  for which the static lattice potential  $U(\mathbf{r}_{nj})$  is a minimum. The following expansions serve as the basis for the present work.

$$U(\mathbf{r}_{nj}) = U(\sigma) = U_0 + \frac{1}{2} \sigma^2 (d^2 U / d\sigma^2)_0 + \dots, \quad (2.10)$$

$$(dU/d\sigma)_0 = 0 \text{ by definition}; \quad (2.11)$$

$$\mathbf{a}_{\mathbf{k}}(\sigma) = (\mathbf{a}_{\mathbf{k}})_0 + \sigma (d\mathbf{a}_{\mathbf{k}}/d\sigma)_0 + \dots. \quad (2.12)$$

Note that in differentiating the  $\mathbf{a}_{\mathbf{k}}$  matrices with respect to  $\epsilon$  (or  $\sigma$ ), the exponential factor can be disregarded since  $\mathbf{k} \cdot \mathbf{r}_{nj}$  is independent of the nearest-neighbor distance.

### Central Potential Models

Calculations were carried out for a model in which all pairs of ions in the crystal interact through the central potential  $\psi(r^2)$ , where  $r$  is the distance between the ions. For this model,<sup>8</sup>

$$A_{\nu i, \nu' i'} = -2[\phi_{\nu\nu'}' \delta_{ii'} + 2\phi_{\nu\nu'}'' (r_{\nu i} - r_{\nu' i})(r_{\nu i'} - r_{\nu' i'})], \quad (2.13)$$

where  $\phi_{\nu\nu}'$  is the first derivative of  $\psi(r^2)$ , with respect to  $r^2$ , evaluated at  $r^2 = (\mathbf{r}_{\nu} - \mathbf{r}_{\nu'})^2$ , and  $\phi_{\nu\nu}''$  is the second derivative. In addition the coefficients  $X_{\nu, i}$  of (2.1) are given by

$$X_{\nu, i} = 2 \sum_{\nu'} \phi_{\nu\nu'}' (r_{\nu i} - r_{\nu' i}), \quad (2.14)$$

where here and in the following the prime on  $\sum'$  means to omit the term  $\nu = \nu'$ . The  $X_{\nu, i}$  vanish by symmetry, and hence vanish for any unit cell volume, for lattices for which the present calculations were carried out. Thus for these lattices with central forces, the equilibrium condition (2.4) is satisfied identically for any unit cell volume.

Two forms for the central potentials were used. These forms lead to the following equations, where the expressions for  $U(\epsilon)$  are restricted to one or two ions per unit cell.

(i) Lennard-Jones (abbreviated LJ):

$$\psi_{\text{LJ}}(r^2) = (A_{\alpha}/r^{\alpha}) - (B_{\beta}/r^{\beta}),$$

where  $A_\alpha, B_\beta, \alpha, \beta$  are positive constants and  $\alpha > \beta$ ,

$$\begin{aligned} U(\epsilon) &= \frac{1}{2}NJ[(A_\alpha S_\alpha/\epsilon^\alpha) - (B_\beta S_\beta/\epsilon^\beta)], \\ \phi_{\nu\nu'} &= \frac{1}{2}[\beta B_\beta (r_{\nu\nu'})^{-(\beta+2)} - \alpha A_\alpha (r_{\nu\nu'})^{-(\alpha+2)}], \\ \phi_{\nu\nu''} &= \frac{1}{4}[\alpha(\alpha+2)A_\alpha (r_{\nu\nu'})^{-(\alpha+4)} \\ &\quad - \beta(\beta+2)B_\beta (r_{\nu\nu'})^{-(\beta+4)}], \end{aligned} \quad (2.15)$$

$$\begin{aligned} (dU/d\sigma)_0 = 0 &\text{ gives } B_\beta = (\alpha S_\alpha/\beta S_\beta)A_\alpha \epsilon_0^{(\beta-\alpha)}, \\ (d^2U/d\sigma^2)_0 &= \frac{1}{2}NJ\alpha(\alpha-\beta)A_\alpha S_\alpha \epsilon_0^{-\alpha}. \end{aligned}$$

(ii) Rydberg (abbreviated  $R$ ):

$$\psi_R(r^2) = -d[1 + \gamma(r-\rho)] \exp[-\gamma(r-\rho)],$$

where  $d, \gamma, \rho$  are positive constants,

$$\begin{aligned} U(\epsilon_0) &= -\frac{1}{2}NJde^{\gamma\rho}[(1-\gamma\rho)R_{0\gamma} + \gamma\epsilon_0 R_{1\gamma}], \\ \phi_{\nu\nu'} &= \frac{1}{2}d\gamma^2 e^{\gamma\rho} [1 - \rho(r_{\nu\nu'})^{-1}] \exp(-\gamma r_{\nu\nu'}), \\ \phi_{\nu\nu''} &= -\frac{1}{4}d\gamma^2 e^{\gamma\rho} [\gamma(r_{\nu\nu'})^{-1} - \gamma\rho(r_{\nu\nu'})^{-2} \\ &\quad - \rho(r_{\nu\nu'})^{-3}] \exp(-\gamma r_{\nu\nu'}), \end{aligned} \quad (2.16)$$

$$(dU/d\sigma)_0 = 0 \text{ gives } \rho/\epsilon_0 = R_{2\gamma}/R_{1\gamma},$$

$$(d^2U/d\sigma^2)_0 = \frac{(\gamma\epsilon_0)^2 [(1+\gamma\rho)R_{2\gamma} - \gamma\epsilon_0 R_{3\gamma}]}{(1-\gamma\rho)R_{0\gamma} + \gamma\epsilon_0 R_{1\gamma}}.$$

The following symbols are used here:

$$r_{\nu\nu'} = |\mathbf{r}_\nu - \mathbf{r}_{\nu'}|, \quad r_\nu = |\mathbf{r}_\nu|, \quad (2.17)$$

$$S_\alpha = \sum_\nu' (\epsilon/r_\nu)^\alpha, \quad (2.18)$$

$$R_{m\gamma} = \sum_\nu' (r_\nu/\epsilon)^m \exp[-\gamma\epsilon_0(r_\nu/\epsilon)]. \quad (2.19)$$

The lattice sums  $S_\alpha, R_{m\gamma}$  are independent of  $\epsilon$ . The defining equations for the lattice vectors are given in Appendix I for fcc, bcc, dia, and hcp lattices. The required lattice sums were calculated in the present work and are tabulated in Appendix II.

All calculations were carried out in terms of reduced quantities, denoted by bars over the corresponding symbols.

$$\begin{aligned} \bar{r}_{\nu\nu'} &= r_{\nu\nu'}/\epsilon, \\ \bar{U} &= U/NJD, \\ \bar{A}_{\nu i, \nu' i'} &= (\epsilon_0^2/D)A_{\nu i, \nu' i'}, \\ \bar{\eta}_{\mathbf{k}s} &= (\epsilon_0^2/D)\eta_{\mathbf{k}s}, \end{aligned} \quad (2.20)$$

where  $D$  is defined by

$$U_0 = -NJD. \quad (2.21)$$

The explicit  $\epsilon$  dependence of  $\phi_{\nu\nu'}, \phi_{\nu\nu''}$  is demonstrated by replacing  $r_{\nu\nu'}$  by  $\epsilon\bar{r}_{\nu\nu'}$ , since  $\bar{r}_{\nu\nu'}$  is independent of  $\epsilon$ .

The reduced dynamical matrices and their first two or three derivatives with respect to  $\sigma$ , all evaluated at  $\sigma=0$ , were computed numerically for  $\mathbf{k}$  vectors in a small portion of the first zone. This portion of the zone (sometimes called the "irreducible" portion) is chosen in such a way that the eigenvalues associated with all

other  $\mathbf{k}$  vectors in the zone are degenerate with the eigenvalues associated with the  $\mathbf{k}$  vectors lying in this portion. The choice of the  $\mathbf{k}$  vectors for each of the four lattice types is described in Appendix I. The method of calculation and the errors have been discussed previously for the  $\mathbf{a}_\mathbf{k}$  matrices at  $\sigma=0$ ; the same procedure was used for the derivative matrices. Then each  $\mathbf{a}_\mathbf{k}(\sigma)$  was calculated according to (2.12), for  $\sigma$  values in the range  $-0.1 \leq \sigma \leq 0.1$ . These matrices were diagonalized by the Jacobi method; for the lattices with two ions per unit cell the  $\mathbf{a}_\mathbf{k}(\sigma)$  were first transformed to real symmetric form.<sup>8</sup> A lattice was considered stable for a particular  $\sigma$  value if, for that  $\sigma$ , every eigenvalue of the dynamical matrix for each chosen  $\mathbf{k}$  was positive. The point  $\mathbf{k}=0$  was not included in the calculations. The numerical work was carried out with the aid of a CDC-1604 digital computer.

The harmonic zero-point energy was computed, in reduced form, for the case where the masses of all the ions are the same, and for each  $\sigma$  value which gave a stable lattice. When all  $M_j=M$ , the eigenvectors are normalized to unity, and

$$\eta_{\mathbf{k}s} = M(\omega_{\mathbf{k}s})^2, \quad \text{all } M_j = M. \quad (2.22)$$

It is convenient to define

$$E_H = (JN)^{-1} \sum_{\mathbf{k}s} \frac{1}{2} \hbar \omega_{\mathbf{k}s}, \quad (2.23)$$

$$\bar{E}_H = E_H/D = \frac{1}{2} \kappa (JN)^{-1} \sum_{\mathbf{k},s} (\bar{\eta}_{\mathbf{k}s})^{1/2}, \quad (2.24)$$

$$\kappa = \hbar/M^{1/2}D^{1/2}\epsilon_0, \quad (2.25)$$

$$F_H = U + NJE_H; \quad \bar{F}_H = F_H/NJD. \quad (2.26)$$

$F_H$  is the Helmholtz free energy at  $T=0$ , neglecting explicit anharmonic contributions. Thus in the quasi-harmonic approximation, the correct value of  $\epsilon$  at zero temperature and pressure is that which minimizes  $F_H(\epsilon)$ . In view of the definition of  $\bar{U}$ , (2.20), it is seen that  $\kappa$  is a dimensionless parameter which relates the importance of the harmonic zero-point energy to the static lattice energy. In calculating  $(\bar{E}_H/\kappa)$ , the sum was carried out over the chosen  $\mathbf{k}$  vectors, with each contribution being multiplied by a weighting factor. The weighting factors were chosen so that each point within the zone would be counted once, and each point on the surface one-half, if a sum were carried out over all the equivalent sets of  $\mathbf{k}$  vectors. The use of such weighting factors greatly improves the accuracy of the sums.<sup>8</sup>

### III. RESULTS

#### Stability

The results of the stability study are summarized in Table I. The Lennard-Jones potential was studied for all four lattices for  $(\alpha, \beta) = (12, 10), (12, 8), (12, 6), (12, 4), (10, 8), (10, 6), (8, 6), (6, 4)$ . The Rydberg potential was studied for bcc as a function of  $\sigma$  and for dia at  $\sigma=0$ . For these lattices the dimensionless parameter  $(\gamma\epsilon_0/\sqrt{3})$

TABLE I. Stability range for each model. The study was carried out for  $-0.1 \leq \sigma \leq 0.1$ . Column 4 lists the order to which the series (2.12) was computed.

Lat-tice	Potential	$\sigma$ incre-ment	Order of (2.12)	Stability range
fcc	LJ all $(\alpha, \beta)$	0.01	$\sigma^2$	-0.1 to 0.1
hcp	LJ all $(\alpha, \beta)$	0.02	$\sigma^2$	-0.1 to 0.1
bcc	{LJ all $(\alpha, \beta)$ except (6,4)}	0.01	$\sigma^3$	none
bcc	LJ (6,4)	0.01	$\sigma^3$	-0.1 to 0.1
bcc	R, $(\gamma\epsilon_0/\sqrt{3})=5$	0.01	$\sigma^2$	none
bcc	R, $(\gamma\epsilon_0/\sqrt{3})=4$	0.01	$\sigma^2$	-0.1 to -0.06
bcc	R, $(\gamma\epsilon_0/\sqrt{3})=3, 2, 1$	0.01	$\sigma^2$	-0.1 to 0.1
dia	LJ (12,10)	0.002	$\sigma^3$	0.002 to 0.032
dia	LJ (12,8)	0.002	$\sigma^3$	0.004 to 0.036
dia	LJ (12,6)	0.002	$\sigma^3$	0.008 to 0.040
dia	LJ (12,4)	0.002	$\sigma^3$	0.012 to 0.048
dia	LJ (10,8)	0.002	$\sigma^3$	0.006 to 0.040
dia	LJ (10,6)	0.002	$\sigma^3$	0.010 to 0.046
dia	LJ (8,6)	0.002	$\sigma^3$	0.014 to 0.052
dia	LJ (6,4)	0.002	$\sigma^3$	0.032 to 0.080

was taken to have the values 5, 4, 3, 2, 1; this range covers the values which have been used previously to discuss the equation of state for several fcc and bcc metals.<sup>6</sup> At  $\sigma=0$ , the dia lattice is not stable for any of the Rydberg potentials.

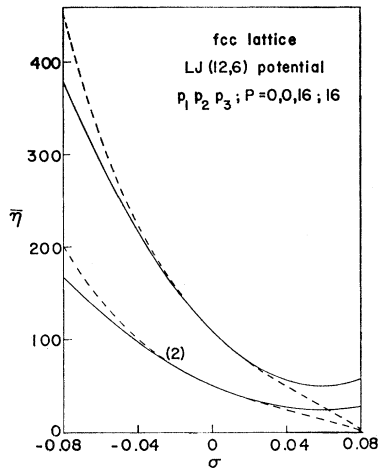


FIG. 1. Variation of  $\bar{\eta}_{ks}$  with  $\sigma$  for fcc, LJ(12,6) potential, for  $\mathbf{k}$  at the point X on the Brillouin zone surface. The lower branch is doubly degenerate.

For bcc, the central force models always give one branch, for  $\mathbf{k}$  along the [011] and nearby directions, for which the eigenvalues are very small in magnitude. When the lattice is unstable the negative eigenvalues lie in this region; in fact for every case in which the bcc lattice is unstable, the matrix for every  $\mathbf{k}$  along the [011] direction has exactly one negative eigenvalue.

The situation is entirely different for the dia lattice. When this lattice is unstable, according to the present potential models, most of the matrices in the Brillouin zone have two negative eigenvalues. For the Lennard-Jones potentials, every matrix in the Brillouin zone has at least one, and usually two, negative eigenvalues for  $-0.1 \leq \sigma \leq 0$ . But every eigenvalue of every matrix is

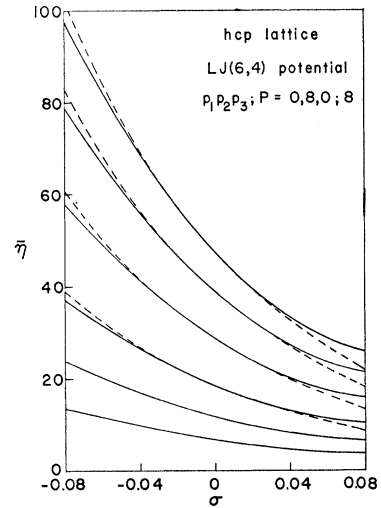


FIG. 2. Variation of  $\bar{\eta}_{ks}$  with  $\sigma$  for hcp, LJ(6,4) potential, for  $\mathbf{k}$  at the point M on the Brillouin zone surface.

positive for a certain range of positive  $\sigma$  values, as listed in Table I.

For a given  $(\mathbf{k}, s)$ ,  $\eta_{ks}$  is expected to decrease in magnitude as  $\sigma$  increases, since the forces of interaction among the ions generally decrease as  $\sigma$  increases. From a study of the  $\eta_{ks}$  as functions of  $\sigma$  for many representative  $\mathbf{k}$  vectors, it appears that all  $|\eta_{ks}|$  decrease with increasing  $\sigma$  for all models which are either stable throughout the range  $-0.1 \leq \sigma \leq 0.1$ , or unstable throughout this range. The variation of  $\eta_{ks}$  with  $\sigma$  is illustrated by several representative graphs, Figs. 1-6. In these graphs the solid lines show the eigenvalues as calculated with the aid of (2.12), and the dashed lines show the limits of error. The dashed line is omitted when the error is too small to be represented on the graph. The errors are due almost entirely to cutting off the series (2.12) after three or four terms; the number of terms taken is the same as that listed in Table I for each model.

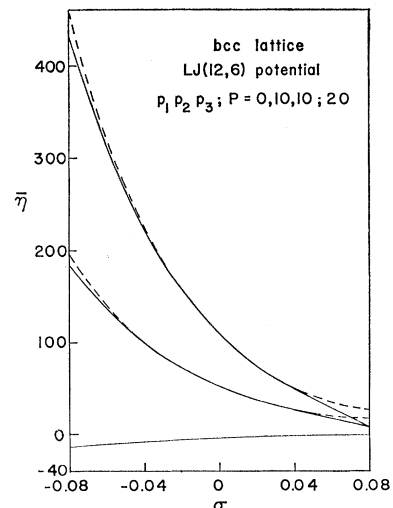


FIG. 3. Variation of  $\bar{\eta}_{ks}$  with  $\sigma$  for bcc, LJ(12,6) potential, for  $\mathbf{k}$  at the point N on the Brillouin zone surface. The lower branch is negative for all  $\sigma$ .

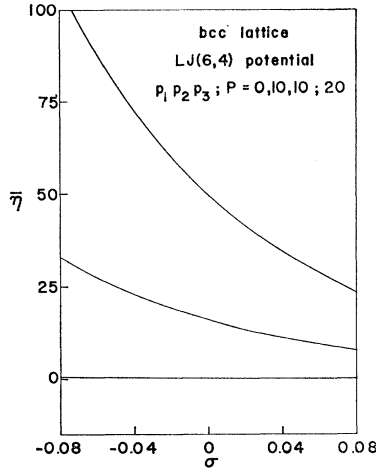


FIG. 4. Variation of  $\bar{\eta}_{ks}$  with  $\sigma$  for bcc, LJ(6,4) potential, for  $\mathbf{k}$  at the point  $N$  on the Brillouin zone surface. The lower branch is positive for all  $\sigma$ .

**Minimization of  $F_H$**

In practically all cases of physical interest, the value of  $\sigma$  for which  $\bar{F}_H$  is a minimum is quite small. It is therefore convenient to express  $\bar{F}_H$  as a Maclaurin series in  $\sigma$ . The coefficients of the appropriate series for  $(\bar{E}_H/\kappa)$ , to order  $\sigma^2$ , were determined from the numerical calculations of  $(\bar{E}_H/\kappa)$  as a function of  $\sigma$ , and are listed in Table II for models which are stable at  $\sigma=0$ . The coefficients are not listed for hcp, since for each Lennard-Jones potential these quantities are the same as for fcc within the following limits: for  $\kappa^{-1}\bar{E}_{H0}$  within 3 parts in  $10^4$  [see Ref. 9, Eq. (4.13)]; for  $\kappa^{-1}(d\bar{E}_H/d\sigma)_0$  within 2 parts in  $10^3$ ; and for  $\kappa^{-1}(d^2\bar{E}_H/d\sigma^2)_0$  within 2 parts in  $10^2$ . The error in  $\kappa^{-1}\bar{E}_H(\sigma)$  as calculated from the data in Table II is less than 0.2% for  $|\sigma| \leq 0.02$ . Figure 7 shows  $(\bar{E}_H/\kappa)$  for the Lennard-Jones (6,4) potential, throughout the range of  $\sigma$  values for which each lattice is stable.

The corresponding series for  $\bar{U}(\sigma)$  is obtained from (2.10) with the aid of (2.15) and (2.16). The series for

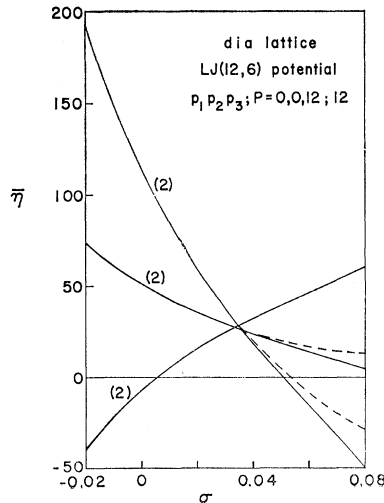


FIG. 5. Variation of  $\bar{\eta}_{ks}$  with  $\sigma$  for dia, LJ(12,6) potential, for  $\mathbf{k}$  at the point  $X$  on the Brillouin zone surface. Each branch is doubly degenerate.

$\bar{F}_H(\sigma)$  is then constructed to order  $\sigma^2$ , and the minimization gives

$$(d\bar{E}_H/d\sigma)_0 + \sigma[(d^2\bar{U}/d\sigma^2)_0 + (d^2\bar{E}_H/d\sigma^2)_0] = 0. \quad (3.1)$$

Equation (3.1) is correct to order  $\sigma$ , and the solution will be denoted by  $\sigma_1$ . It is seen that  $\sigma_1$  for a given lattice and potential model depends on  $\kappa$ . The values of  $\kappa$  have been calculated for most elements in the solid state; some representative values are listed in Table III. For these calculations  $D$  has been taken to be the measured binding energy per atom, evaluated at  $T=0$  where possible, and  $\epsilon_0$  the observed nearest-neighbor distance at room temperature. For most elements,  $(10^3)\kappa$  lies in the range 0.5 to 5.0.

Since  $\kappa$  is small, it is useful to carry out further expansions in powers of  $\kappa$ . Thus, with the aid of (3.1),

$$\begin{aligned} \sigma_1 &= c_1\kappa + c_2\kappa^2 + \dots, \\ c_1 &= -[\kappa^{-1}(d\bar{E}_H/d\sigma)_0]/(d^2\bar{U}/d\sigma^2)_0, \text{ etc.}; \end{aligned} \quad (3.2)$$

$$\begin{aligned} \bar{F}_H(\sigma_1) &= -1 + c_3\kappa + c_4\kappa^2 + \dots, \\ c_3 &= \kappa^{-1}\bar{E}_{H0}, \text{ etc.} \end{aligned} \quad (3.3)$$

The coefficients  $c_1, \dots$ , are determined in a straight-

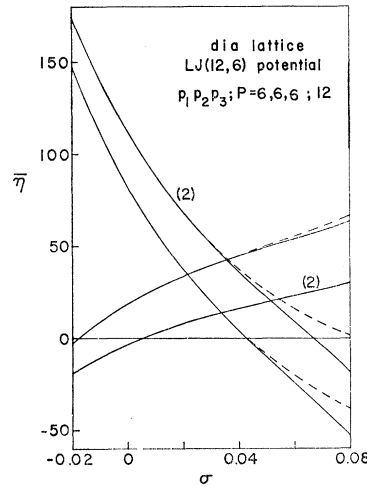


FIG. 6. Variation of  $\bar{\eta}_{ks}$  with  $\sigma$  for dia, LJ(12,6) potential, for  $\mathbf{k}$  at the point  $L$  on the Brillouin zone surface. The two branches marked (2) are each doubly degenerate.

forward way from preceding equations. For the central force models which are stable at  $\sigma=0$ , the  $c_1$  are all in the range  $1.15 \pm 0.25$ ; these values are listed in Table II. For  $\kappa=5(10^{-3})$ , the contribution of terms of order  $\kappa^2$  and higher in (3.2) is  $\leq 5\%$  for the models listed in Table II. In (3.3) the first term is the reduced static-lattice potential energy at  $\sigma=0$ , the second term is the reduced harmonic zero-point energy at  $\sigma=0$ , and the remaining terms are corrections due to  $\sigma_1 \neq 0$ . For  $\kappa=5(10^{-3})$ , the contribution of terms of order  $\kappa^2$  and higher in (3.3) is  $\leq 0.2\%$  for the models listed in Table II. For  $\kappa < 5(10^{-3})$ , the contributions of the higher order terms in (3.2) and (3.3) are correspondingly smaller.

The variation of  $(\bar{E}_H/\kappa)$  with  $\sigma$  for dia with the

TABLE II. Coefficients of the series for  $(\bar{E}_H/\kappa)$  for small  $\sigma$ , and values of  $c_1$ , Eq. (3.2). Each value is accurate to 1 part in  $10^n$  when  $n+1$  significant figures are given.

Lattice	Potential	$\kappa^{-1}\bar{E}_{H0}$	$\kappa^{-1}(d\bar{E}_H/d\sigma)_0$	$\kappa^{-1}(d^2\bar{E}_H/d\sigma^2)_0$	$c_1$
fcc	LJ (12,10)	13.12	-146.7	12.2(10 <sup>2</sup> )	1.22
fcc	LJ (12,8)	11.82	-119.4	9.57(10 <sup>2</sup> )	1.24
fcc	LJ (12,6)	10.38	-93.15	7.20(10 <sup>2</sup> )	1.29
fcc	LJ (12,4)	8.698	-67.10	5.26(10 <sup>2</sup> )	1.40
fcc	LJ (10,8)	10.87	-98.60	7.23(10 <sup>2</sup> )	1.23
fcc	LJ (10,6)	9.567	-75.90	5.27(10 <sup>2</sup> )	1.27
fcc	LJ (8,6)	8.691	-59.70	3.74(10 <sup>2</sup> )	1.24
fcc	LJ (6,4)	6.597	-30.44	1.58(10 <sup>2</sup> )	1.27
bcc	LJ (6,4)	6.332	-29.24	1.52(10 <sup>2</sup> )	1.22
bcc	R, ( $\gamma\epsilon_0/\sqrt{3}$ )=3	6.794	-27.62	0.782(10 <sup>2</sup> )	0.962
bcc	R, ( $\gamma\epsilon_0/\sqrt{3}$ )=2	5.269	-12.71	0.249(10 <sup>2</sup> )	0.960
bcc	R, ( $\gamma\epsilon_0/\sqrt{3}$ )=1	3.681	-4.297	0.0560(10 <sup>2</sup> )	1.05

Lennard-Jones (6,4) potential, Fig. 7, is representative of the behavior for the other Lennard-Jones potentials for dia. The minimization of  $\bar{F}_H(\sigma)$  for dia was studied graphically, and it was found that for  $\kappa \leq (10^{-2})$  there is no minimum in  $\bar{F}_H(\sigma)$  in the range of  $\sigma$  for which the lattice is stable for any of the Lennard-Jones potentials.

 TABLE III.  $\kappa$  values for some elements.

Element	Structure	(10 <sup>3</sup> ) $\kappa$	Element	Structure	(10 <sup>3</sup> ) $\kappa$
Ne	fcc	33.5	Si	dia	2.67
Ar	fcc	9.62	Ge	dia	1.68
Kr	fcc	5.25	Cu	fcc	1.69
Xe	fcc	3.22	Ag	fcc	1.25
Li	bcc	6.42	Au	fcc	0.846
Na	bcc	3.41	Pb	fcc	0.904
K	bcc	2.31	Th	fcc	0.426
Rb	bcc	1.50	Be	hcp	5.24
Cs	bcc	1.17	Mg	hcp	3.28
C	dia	4.45	Gd	hcp	0.737

### Application to Inert-Gas Crystals

In a previous paper<sup>9</sup> the contributions to the static-lattice potential energy, the harmonic zero-point energy,

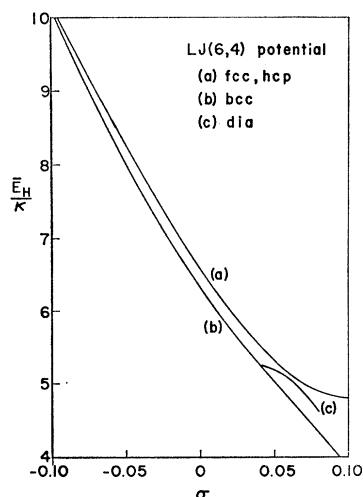


FIG. 7. Variation of  $(\bar{E}_H/\kappa)$  with  $\sigma$  for fcc, hcp, bcc, and dia lattices for LJ(6,4) potential. The fcc and hcp are indistinguishable on the graph [line (a)].

and the anharmonic zero-point energy, all at  $\sigma=0$ , were calculated for the inert gas crystals in the fcc and hcp lattices. These calculations were based on a Lennard-Jones (12,6) potential, with the constants  $A_\alpha, B_\beta$  of (2.15) being determined from the data in Appendix II of the article by Dobbs and Jones.<sup>10</sup> For the specified potential (Table V of Ref. 9) it is appropriate to calculate  $\kappa$  from the calculated values of  $D$  and  $\epsilon_0$ , rather than from the measured values. This has been done for the fcc lattice, and the results are listed in Table IV.

 TABLE IV. Application to the inert-gas crystals in the fcc lattice.  $\epsilon_0(1+\sigma_1)$  is in Å, and all energy contributions are in cal/mole.

Element	(10 <sup>3</sup> ) $\kappa$	(10 <sup>3</sup> ) $\sigma_1$	$\epsilon_0(1+\sigma_1)$	$F_H(\sigma=0)$	$F_H(\sigma_1)$	$L_0$
Ne	29.5	32.5±0.5	3.10	-423	-449	426
Ar	9.14	12.0±0.5	3.75	-1898	-1908	1900
Kr	5.02	6.2±0.3	4.03	-2693	-2697	2694
Xe	3.11	3.9±0.2	4.46	-3724	-3726	3724

Also for fcc,  $\bar{F}_H(\sigma)$  has been minimized graphically since  $\kappa$  is large for the inert gas crystals; the results are listed in Table IV. In addition, Table IV lists the total calculated binding energy  $L_0$  of the crystals at  $T=0$ :

$$L_0 = -[F_H(\sigma_1) + F_{A0}], \quad (3.4)$$

where  $F_{A0}$ , the anharmonic zero-point energy, is taken from Table V of Ref. 9.

It is seen that the nearest-neighbor distance  $\epsilon_0(1+\sigma_1)$ , as determined from minimizing  $F_H$ , is in somewhat better agreement with the observed value than is  $\epsilon_0$  (compare Table V, Ref. 9). In addition it is seen that the contributions to the total energy at  $T=0$  arising from anharmonicity ( $F_{A0}$ ) and arising from  $\sigma_1 \neq 0$  [ $F_H(\sigma_1) - F_H(0)$ ] are of opposite sign and nearly cancel one another. Further calculations are in progress to test the generality of this finding.

A comparison of the fcc and hcp lattices for the

<sup>10</sup> E. R. Dobbs and G. O. Jones, Rept. Progr. Phys. 20, 516 (1957).

LJ (12,6) potential shows that the minimization of  $F_H(\sigma)$  increases the binding energy of hcp more than fcc by  $5(10^{-4})\%$  of the total binding energy for Ne,  $5(10^{-5})\%$  for Ar,  $2(10^{-5})\%$  for Kr, and  $5(10^{-6})\%$  for Xe.

#### IV. DISCUSSION

The present lattice dynamics calculations have been carried out for varying values of the nearest-neighbor distance  $\epsilon$  by means of Maclaurin series in  $\sigma$ . For all  $\sigma$  values, the equilibrium condition is satisfied for central potential models for the lattices considered here. At  $\sigma=0$ , the static lattice potential is stationary with respect to variation of  $\sigma$ . It can be shown that this implies that the static lattice potential is stationary with respect to arbitrary homogeneous deformation of the lattice at  $\sigma=0$ , for fcc, bcc, and dia with arbitrary central potentials. This is also true for hcp with arbitrary central potentials when only first and second neighbors are taken into account, but not when further neighbors are included. The second equilibrium condition of Born and Huang,<sup>4</sup> namely that the stresses must vanish in the equilibrium configuration, is therefore satisfied only at  $\sigma=0$  for fcc, bcc, and dia for the models of the present paper. This circumstance causes no difficulty; when the second condition is not satisfied it simply means that the lattice model approximates a crystal which has surface forces applied by external means.

An interesting result of the present stability study is that any model which is stable at  $\sigma=0$  is also stable throughout the range  $-0.1 \leq \sigma \leq 0.1$ . The close packed lattices are stable for all potential models studied, throughout the  $\sigma$  range studied. The bcc lattice is generally unstable for short-range central forces, but stable throughout the  $\sigma$  range studied for long-range central forces. In spite of the fact that bcc and dia are both stable for certain central potentials and certain  $\sigma$  values, the central potential models are quite inappropriate for the quantitative representation of a real crystal with either of these structures. For bcc, one branch of eigenvalues for  $\mathbf{k}$  along the [011] direction is very small for all the models (see Figs. 3, 4), while for dia there is no minimum in  $F_H(\sigma)$ , for any physically reasonable value of  $\kappa$  for any of the Lennard-Jones potentials studied here, in the  $\sigma$  range for which the lattice is stable.

For all stable models except dia, the eigenvalues  $\eta_{ks}$  were found to decrease with increasing  $\sigma$  as expected. Thus the Gruneisen parameters  $\gamma_{ks}$ , defined by

$$\gamma_{ks} = -d \ln \omega_{ks} / d \ln V,$$

are in general positive and the thermal expansion for such a model is in general positive. Aside from questions of the validity of the model, it is interesting to note that for dia, for all Lennard-Jones potentials studied and in the stable  $\sigma$  range, every dynamical matrix has at least one and usually two acoustic eigenvalues which

increase with increasing  $\sigma$  (see Figs. 5, 6). Thus it is quite likely that the thermal expansion for dia for the central potential models would be negative, especially at low temperatures. Negative thermal expansion coefficients have been observed for materials crystallizing in the dia structure.<sup>11</sup>

Born<sup>1</sup> has suggested that if a lattice is stable for long waves, it is also stable for short waves. For the models of the present paper, this is true for fcc, bcc, and hcp, but not for dia. For the Lennard-Jones (12,6) potential for dia, there is a narrow range of  $\sigma$  values just below the stable  $\sigma$  range for which all long wavelength normal modes have real frequencies while some of the short wavelength acoustic modes have imaginary frequencies. The same result appears to hold for the other potentials studied for dia. This conclusion is based on the behavior for a limited number of  $\mathbf{k}$  vectors in the Brillouin zone. All possible long wavelength modes can be included by constructing the elastic energy density with the aid of the lattice sums of Appendix II; this has not been done in the present work.

With regard to the minimization of  $F_H(\sigma)$ , it is found that for all models stable at  $\sigma=0$  and for any  $\kappa \leq 5(10^{-3})$ ,  $\sigma_1$  lies in the range  $(1.15 \pm 0.25)\kappa$ , including all errors. It is therefore suggested that  $\sigma_1 \approx \kappa$  is a good approximation for the relative change in the nearest-neighbor distance, at zero temperature and pressure, due to the effect of harmonic zero-point motion, for most physically reasonable models.

#### APPENDIX I: LATTICE VECTORS AND WAVE VECTORS

The lattice sites are defined in terms of unit vectors and the coefficients  $n_1, n_2, n_3$ , which are integers (including zero). The  $\mathbf{k}$  vectors are similarly defined in terms of unit vectors and the coefficients  $p_1, p_2, p_3$ , which are integers. The restrictions on these two sets of integers are given here.  $\mathbf{x}, \mathbf{y}$ , and  $\mathbf{z}$  are unit Cartesian vectors and  $P$  is a positive number.

##### fcc Lattice

$$\begin{aligned} \mathbf{r}_n &= (\epsilon/\sqrt{2})(n_1\mathbf{x} + n_2\mathbf{y} + n_3\mathbf{z}), \\ n_1 + n_2 + n_3 &= \text{even integer (including zero)}, \\ \mathbf{k}_p &= (\sqrt{2}\pi/\epsilon P)(p_1\mathbf{x} + p_2\mathbf{y} + p_3\mathbf{z}). \end{aligned}$$

For  $\mathbf{k}_p$  lying in (1/48) of the first zone,

$$\begin{aligned} 0 &\leq p_3 \leq P, \\ 0 &\leq p_2 \leq p_2', \quad p_2' = \text{minimum of } (p_3, \frac{2}{3}P - p_3), \\ 0 &\leq p_1 \leq p_1', \quad p_1' = \text{minimum of } (p_2, \frac{2}{3}P - p_3 - p_2). \end{aligned}$$

The final calculations were done for  $P=16$ , corresponding to 504 points in (1/48) of the zone, or to 16 431 distinct points in the entire zone, not counting  $\mathbf{k}_p=0$ .

<sup>11</sup> D. F. Gibbons, Phys. Rev. **112**, 136 (1958).

TABLE V. Lattice sums of the power type. When  $n+1$  significant figures are given, the error is no more than 1 part in  $10^n$ .

$\alpha$	fcc lattice		bcc lattice		$S_\alpha$	dia lattice		$S_\alpha$	hcp lattice		
	$S_\alpha$	$S_{\alpha zzz}$	$S_\alpha$	$S_{\alpha zzz}$		$S_{\alpha yz}$	$S_{\alpha zzz}$		$S_{\alpha z}$	$S_{\alpha zy}$	$S_{\alpha zzz}$
4	25.338304	4.79210	22.638722	4.22881	10.232845	0.720095	1.66902	25.339080	8.44875	0.175124	5.25765
5	16.9675185	3.089418	14.7585093	2.605810	6.31276034	0.7414699	0.8903750	16.9684363	5.658396	0.199622	3.601729
6	14.4539211	2.563592	12.2536679	2.061402	5.11677158	0.7539560	0.6559089	14.4548973	4.820331	0.2200549	3.113532
7	13.3593877	2.326452	11.0542435	1.782002	4.59447603	0.7610725	0.5551497	13.3603468	4.455195	0.2365781	2.905902
8	12.8019372	2.200869	10.3551979	1.606707	4.33191374	0.7650495	0.5053371	12.8028219	4.269046	0.2496107	2.803005
9	12.4925467	2.128277	9.89458966	1.483018	4.19037213	0.7672383	0.4789120	12.4933217	4.165586	0.2596846	2.747578
10	12.3112457	2.083982	9.56440061	1.389101	4.11102360	0.7684288	0.4643147	12.3118962	4.104851	0.2673447	2.716107
11	12.2009204	2.055958	9.31326254	1.314379	4.06546760	0.7690702	0.4560443	12.2014471	4.067817	0.2730921	2.697565
12	12.1318802	2.037770	9.11418327	1.253128	4.03890471	0.7694134	0.4512781	12.1322938	4.044590	0.2773576	2.686333
13	12.0877263	2.025742	8.95180732	1.201947	4.02325119	0.7695960	0.4484981	12.0880426	4.029704	0.2804952	2.679375
14	12.0589920	2.017677	8.81677023	1.158651	4.01395609	0.7696927	0.4468619	12.0592283	4.019996	0.2827864	2.674985
15	12.0400241	2.012209	8.70298456	1.121731	4.00840524	0.7697438	0.4458924	12.0401971	4.013577	0.2844497	2.672171
16	12.0273549	2.008472	8.60625405	1.090085	4.00507587	0.7697706	0.4453147	12.0274794	4.009283	0.2856513	2.670344
17	12.0188094	2.005900	8.52353125	1.062866	4.00307204	0.7697848	0.4449690	12.0188977	4.006383	0.2865159	2.669143
18	12.0129983	2.004121	8.45250317	1.039402	4.00186265	0.7697922	0.4447614	12.0130600	4.004410	0.2871361	2.668346
19	12.0090196	2.002885	8.39135079	1.019145	4.00113108	0.7697961	0.4446363	12.0090622	4.003059	0.2875797	2.667812
20	12.0062800	2.002023	8.33860401	1.001639	4.00068771	0.7697981	0.4445608	12.0063092	4.002129	0.2878964	2.667452
30	12.0001848	2.000061	8.08018575	0.9156166	4.00000494	0.7698004	0.4444453	12.0001852	4.000062	0.2886503	2.666688
$\infty$	12	2	8	(8/9)	4	(4/3√3)	(4/9)	12	4	(√3/6)	(8/3)

**bcc Lattice**

$$\mathbf{r}_n = (\epsilon/\sqrt{3})(n_1\mathbf{x} + n_2\mathbf{y} + n_3\mathbf{z}),$$

$n_1, n_2, n_3$  are either all even or all odd,

$$\mathbf{k}_p = (\sqrt{3}\pi/\epsilon P)(p_1\mathbf{x} + p_2\mathbf{y} + p_3\mathbf{z}).$$

For  $\mathbf{k}_p$  lying in (1/48) of the first zone,

$$0 \leq p_3 \leq P,$$

$$0 \leq p_2 \leq p_2', p_2' = \text{minimum of } (p_3, P - p_3),$$

$$0 \leq p_1 \leq p_2.$$

The final calculations were done for  $P=20$ , corresponding to 505 points in (1/48) of the zone, or to 16 039 distinct points in the entire zone, not counting  $\mathbf{k}_p=0$ .

**dia Lattice**

$\mathbf{r}_n$  = primitive lattice points,

$$\mathbf{r}_n = (2\epsilon/\sqrt{3})(n_1\mathbf{x} + n_2\mathbf{y} + n_3\mathbf{z}),$$

$n_1 + n_2 + n_3$  = even integer (including zero),

$$\text{basis vector} = (\epsilon/\sqrt{3})(\mathbf{x} + \mathbf{y} + \mathbf{z}),$$

$$\mathbf{k}_p = (\sqrt{3}\pi/2\epsilon P)(p_1\mathbf{x} + p_2\mathbf{y} + p_3\mathbf{z}).$$

For  $\mathbf{k}_p$  lying in (1/48) of the first zone, the rules are the same as for fcc. The final calculations were done for  $P=12$ , corresponding to 239 points in (1/48) of the zone, or 6947 distinct points in the entire zone, not counting  $\mathbf{k}_p=0$ .

**hcp Lattice**

$\mathbf{b}_1, \mathbf{b}_2, (\frac{2}{3})^{1/2}\mathbf{b}_3$  are unit vectors in a simple hexagonal coordinate system, related to the Cartesian system

according to

$$\mathbf{x} = (\mathbf{b}_1 + \mathbf{b}_2), \mathbf{y} = (3)^{-1/2}(\mathbf{b}_2 - \mathbf{b}_1), \mathbf{z} = (\frac{3}{8})^{1/2}\mathbf{b}_3.$$

$\mathbf{r}_n$  = primitive lattice points,

$$\mathbf{r}_n = \epsilon(n_1\mathbf{b}_1 + n_2\mathbf{b}_2 + n_3\mathbf{b}_3),$$

basis vector =  $\epsilon(\frac{1}{3}\mathbf{b}_1 + \frac{2}{3}\mathbf{b}_2 + \frac{1}{2}\mathbf{b}_3)$ ,

$$\mathbf{k}_p = (\pi/\epsilon P)(p_1\mathbf{c}_1 + p_2\mathbf{c}_2 + p_3\mathbf{c}_3),$$

where  $\mathbf{c}_i \cdot \mathbf{b}_j = \delta_{ij}$  defines the  $\mathbf{c}_i$ .

For  $\mathbf{k}_p$  lying in (1/24) of the first zone,

$$0 \leq p_3 \leq P,$$

$$0 \leq p_2 \leq P,$$

$$0 \leq p_1 \leq p_1', p_1' = \text{minimum of } (p_2, 2P - 2p_2).$$

The final calculations were done for  $P=8$ , corresponding to 269 points in (1/24) of the zone, or to 4110 distinct points in the entire zone, not counting  $\mathbf{k}_p=0$ . Note that the above restrictions give  $\mathbf{k}_p$  lying in (1/24) of the zone, while the similar restrictions in Ref. 8 give  $\mathbf{k}_p$  lying in ( $\frac{1}{8}$ ) of the zone.

**APPENDIX II: LATTICE SUMS**

The lattice sums needed in the present and previous investigations,<sup>8,9</sup> and also the sums needed for the calculation of elastic constants for these central force models, are listed in Tables V and VI. These sums are defined as follows, with an obvious notation.

$$S_\alpha = \sum_{\nu'} (\bar{r}_\nu)^{-\alpha},$$

$$S_{\alpha z z} = \sum_{\nu'} (\bar{r}_{\nu z})^2 (\bar{r}_\nu)^{-(\alpha+2)} \text{ etc.};$$

$$R_{m\gamma} = \sum_{\nu'} (\bar{r}_\nu)^m \exp(-\gamma\epsilon_0\bar{r}_\nu),$$

$$R_{m\gamma z z} = \sum_{\nu'} (\bar{r}_{\nu z})^2 (\bar{r}_\nu)^{(m-2)} \exp(-\gamma\epsilon_0\bar{r}_\nu) \text{ etc.}$$

These sums were calculated by direct summation over all lattice points in a large sphere, with a remainder



TABLE VI. Lattice sums of the exponential type. When  $n+1$  significant figures are given, the error is no more than 1 part in  $10^n$ .

$(\gamma\epsilon_0/\sqrt{3})$	$m$	bcc lattice		dia lattice
		$R_{m\gamma}$	$R_{m\gamma zzzz}$	$R_{m\gamma}$
1	0	5.66966120	1.101532	2.66064301
1	1	10.6835928	2.113533	5.20842126
1	2	25.0948013	5.004281	12.4733493
1	3	72.5645043	14.50538	36.2762856
1	4		50.26584	
2	0	4.53971096(10 <sup>-1</sup> )	0.8214568(10 <sup>-1</sup> )	1.89190797(10 <sup>-1</sup> )
2	1	5.54581936(10 <sup>-1</sup> )	1.039539(10 <sup>-1</sup> )	2.40400020(10 <sup>-1</sup> )
2	2	7.43792674(10 <sup>-1</sup> )	1.435327(10 <sup>-1</sup> )	3.39071947(10 <sup>-1</sup> )
2	3	11.2759740(10 <sup>-1</sup> )	2.220013(10 <sup>-1</sup> )	5.39385277(10 <sup>-1</sup> )
2	4		3.919647(10 <sup>-1</sup> )	
3	0	6.31844144(10 <sup>-2</sup> )	1.061355(10 <sup>-2</sup> )	2.52777813(10 <sup>-2</sup> )
3	1	6.85626140(10 <sup>-2</sup> )	1.195587(10 <sup>-2</sup> )	2.74831007(10 <sup>-2</sup> )
3	2	7.68304371(10 <sup>-2</sup> )	1.390091(10 <sup>-2</sup> )	3.13326823(10 <sup>-2</sup> )
3	3	9.03311393(10 <sup>-2</sup> )	1.691268(10 <sup>-2</sup> )	3.81634435(10 <sup>-2</sup> )
3	4		2.191750(10 <sup>-2</sup> )	
4	0	1.00483800(10 <sup>-2</sup> )	1.577022(10 <sup>-3</sup> )	4.08735995(10 <sup>-3</sup> )
4	1	1.05008748(10 <sup>-2</sup> )	1.706439(10 <sup>-3</sup> )	4.20061843(10 <sup>-3</sup> )
4	2	1.11067430(10 <sup>-2</sup> )	1.871417(10 <sup>-3</sup> )	4.39217241(10 <sup>-3</sup> )
4	3	1.19562332(10 <sup>-2</sup> )	2.090116(10 <sup>-3</sup> )	4.71833186(10 <sup>-3</sup> )
4	4		2.394560(10 <sup>-3</sup> )	
5	0	1.66955181(10 <sup>-3</sup> )	2.467008(10 <sup>-4</sup> )	7.02788180(10 <sup>-4</sup> )
5	1	1.71882845(10 <sup>-3</sup> )	2.620120(10 <sup>-4</sup> )	7.08980718(10 <sup>-4</sup> )
5	2	1.77964909(10 <sup>-3</sup> )	2.804026(10 <sup>-4</sup> )	7.19305390(10 <sup>-4</sup> )
5	3	1.85669222(10 <sup>-3</sup> )	3.028840(10 <sup>-4</sup> )	7.36581077(10 <sup>-4</sup> )
5	4		3.310464(10 <sup>-4</sup> )	

added to account for points lying outside the sphere. Convergence studies were carried out to determine the accuracy of the sums. Each tabulated value is in error by no more than 1 part in  $10^n$  when  $n+1$  significant figures are given.

The lattice symmetry gives rise to certain relations between the sums. For fcc, bcc, and dia

$$\begin{aligned} S_{\alpha xx} &= S_{\alpha yy} = S_{\alpha zz} = \frac{1}{3} S_{\alpha}, \\ S_{\alpha zzzz} &= S_{\alpha yyy} = S_{\alpha xxx}, \\ S_{\alpha xxyy} &= S_{\alpha zzzz} = S_{\alpha yyzz}, \\ 3S_{\alpha zzzz} + 6S_{\alpha xxyy} &= S_{\alpha}. \end{aligned}$$

All other sums with up to four Cartesian indices vanish for fcc and bcc, while for dia there is only one other nonvanishing sum, namely  $S_{\alpha xyz}$ . The contribution to  $S_{\alpha xyz}$  for dia vanishes for the primitive points, but not for the basis points.

For hcp

$$\begin{aligned} S_{\alpha xx} &= S_{\alpha yy} \neq S_{\alpha zz}, \\ S_{\alpha xx} &= \frac{1}{2} [S_{\alpha} - S_{\alpha zz}], \\ S_{\alpha zzzz} &= S_{\alpha yyy} \neq S_{\alpha xxx}, \\ S_{\alpha zzzz} &= S_{\alpha yyzz} \neq S_{\alpha xxyy}, \\ S_{\alpha zzzz} &= \frac{1}{2} [S_{\alpha zz} - S_{\alpha xxx}], \\ S_{\alpha xxyy} &= \frac{1}{8} [S_{\alpha} - 2S_{\alpha zz} + S_{\alpha zzzz}], \\ S_{\alpha zzzz} &= 3S_{\alpha xxyy}. \end{aligned}$$

Thus it is only necessary to know  $S_{\alpha}$ ,  $S_{\alpha zz}$ , and  $S_{\alpha zzzz}$  in order to calculate all the other sums defined above for hcp. There is one more nonvanishing sum for hcp with up to four Cartesian indices, namely  $S_{\alpha xxyy} = -S_{\alpha yyy}$ . Again the contribution to this sum vanishes for primitive points but not for basis points. An analogous set of relations hold, for each lattice, for the  $R_{m\gamma}$ ,  $R_{m\gamma zz}$  etc.

The results in Tables V and VI are more accurate than previous tabulations. The previous work includes values of  $S_{\alpha}$  for primitive cubic lattices,<sup>12</sup> values of  $S_{\alpha}$  and  $S_{\alpha zzzz}$  for primitive cubic lattices,<sup>2</sup> some values of  $S_{\alpha}$ ,  $S_{\alpha zz}$ , and  $S_{\alpha zzzz}$  for hcp,<sup>13</sup> some values of  $S_{\alpha}$  for fcc and hcp,<sup>14,15</sup> accurate differences between  $S_{\alpha}$  for hcp and fcc,<sup>16</sup> and some exponential-type sums for fcc and bcc.<sup>17</sup>

<sup>12</sup> J. E. Jones and A. E. Ingham, Proc. Roy. Soc. (London) A107, 636 (1925).

<sup>13</sup> G. Kane and M. Goepfert-Mayer, J. Chem. Phys. 8, 642 (1940).

<sup>14</sup> J. A. Prins, J. M. Dumore, and L. T. Tjoan, Physica 18, 307 (1952).

<sup>15</sup> T. Kihara and S. Koba, J. Phys. Soc. Japan 7, 348 (1952).

<sup>16</sup> T. H. K. Barron and C. Domb, Proc. Roy. Soc. (London) A227, 447 (1955).

<sup>17</sup> L. A. Girifalco and V. G. Weizer, NASA Technical Report R-5 (unpublished).